blood®
Regular Article

MYELOID NEOPLASIA

Secreted mutant calreticulins as rogue cytokines in myeloproliferative neoplasms

Christian Pecquet,[1,2,*] Nicolas Papadopoulos,[1,2,*] Thomas Balligand,[1,2,*] Ilyas Chachoua,[1-3,*] Amandine Tisserand,[4-6,*] Gaëlle Vertenoeil,[1,2] Audrey Nédélec,[1,2] Didier Vertommen,[2] Anita Roy,[1,2] Caroline Marty,[4,6,7] Harini Nivarthi,[8] Jean-Philippe Defour,[1,2] Mira El-Khoury,[4,6,7] Eva Hug,[9] Andrea Majoros,[9] Erica Xu,[9] Oleh Zagrijtschuk,[10] Tudor E. Fertig,[10] Daciana S. Marta,[11] Heinz Gisslinger,[12] Bettina Gisslinger,[12] Martin Schalling,[12] Ilaria Casetti,[13] Elisa Rumi,[13] Daniela Pietra,[13] Chiara Cavalloni,[13] Luca Arcaini,[13] Mario Cazzola,[13] Norio Komatsu,[14] Yoshihiko Kihara,[14] Yoshitaka Sunami,[14] Yoko Edahiro,[14] Marito Araki,[15] Roman Lesyk,[16,17] Veronika Buxhofer-Ausch,[18,19] Sonja Heibl,[20] Florence Pasquier,[4-6,21] Violaine Havelange,[2,22] Isabelle Plo,[4,6,7] William Vainchenker,[4,6,7] Robert Kralovics,[23] and Stefan N. Constantinescu[1,2,24,25]

[1]Ludwig Cancer Research, Brussels, Belgium; [2]Université Catholique de Louvain and de Duve Institute, SIGN Unit, Brussels, Belgium; [3]Department of Molecular Biology and Genetics, Bilkent University, Ankara, Turkey; [4]INSERM, Unité Mixte de Recherche (UMR) 1287, Gustave Roussy, Villejuif, France; [5]Université Paris Cité, UMR 1287, Gustave Roussy, Villejuif, France; [6]UMR 1287, Gustave Roussy, Villejuif, France; [7]Université Paris-Saclay, UMR 1287, Gustave Roussy, Villejuif, France; [8]CeMM Research Center for Molecular Medicine of the Austrian Academy of Sciences, Vienna, Austria; [9]MyeloPro Diagnostics and Research GmbH, Vienna, Austria; [10]MyeloPro Diagnostics and Research GmbH, Vienna, Austria; [11]Ultrastructural Pathology Lab and Bioimaging, Institute of Pathology Victor Babeș, Bucharest, Romania; [12]Division of Hematology and Blood Coagulation, Department of Internal Medicine I, Division of Hematology and Blood Coagulation, Medical University of Vienna, Vienna, Austria; [13]Division of Hematology, Fondazione IRCCS Policlinico San Matteo and University of Pavia, Pavia, Italy; [14]Department of Hematology and [15]Department of Transfusion Medicine and Stem Cell Regulation, Graduate School of Medicine, Juntendo University, Tokyo, Japan; [16]Department of Biotechnology and Cell Biology, Medical College, University of Information Technology and Management in Rzeszow, Rzeszow, Poland; [17]Department of Pharmaceutical, Organic and Bioorganic Chemistry, Danylo Halytsky Lviv National Medical University, Lviv, Ukraine; [18]Department of Internal Medicine I with Hematology, Ordensklinikum Linz Elisabethinen, Stem Cell Transplantation Hemostaseology and Medical Oncology, Linz, Austria; [19]Medical Faculty, Johannes Kepler University Linz, Linz, Austria; [20]Department of Internal Medicine IV, Klinikum Wels-Grieskirchen, Wels, Austria; [21]Department of Hematology, Gustave Roussy, Villejuif, France; [22]Department of Hematology, Cliniques universitaires Saint-Luc, Brussels, Belgium; [23]Department of Laboratory Medicine, Medical University of Vienna, Vienna, Austria; [24]Walloon Excellence in Life Sciences and Biotechnology, Brussels, Belgium; and [25]Ludwig Institute for Cancer Research, Nuffield Department of Medicine, Oxford University, Oxford, United Kingdom

KEY POINTS

- **Mutant CALR proteins are secreted in complex with sTFR1 to the plasma of MPN patients and activate the TpoR in a rogue cytokine fashion.**
- **TpoR-expressing cells with a *CALR* mutation are uniquely sensitive to the levels of circulating mutant CALR proteins seen in patients.**

Mutant calreticulin (CALR) proteins resulting from a −1/+2 frameshifting mutation of the *CALR* exon 9 carry a novel C-terminal amino acid sequence and drive the development of myeloproliferative neoplasms (MPNs). Mutant CALRs were shown to interact with and activate the thrombopoietin receptor (TpoR/MPL) in the same cell. We report that mutant CALR proteins are secreted and can be found in patient plasma at levels up to 160 ng/mL, with a mean of 25.64 ng/mL. Plasma mutant CALR is found in complex with soluble transferrin receptor 1 (sTFR1) that acts as a carrier protein and increases mutant CALR half-life. Recombinant mutant CALR proteins bound and activated the TpoR in cell lines and primary megakaryocytic progenitors from patients with mutated *CALR* in which they drive thrombopoietin-independent colony formation. Importantly, the CALR-sTFR1 complex remains functional for TpoR activation. By bioluminescence resonance energy transfer assay, we show that mutant CALR proteins produced in 1 cell can specifically interact in trans with the TpoR on a target cell. In comparison with cells that only carry TpoR, cells that carry both TpoR and mutant CALR are hypersensitive to exogenous mutant CALR proteins and respond to levels of mutant CALR proteins similar to those in patient plasma. This is consistent with CALR-mutated cells that expose TpoR carrying immature N-linked sugars at the cell surface. Thus, secreted mutant CALR proteins will act more specifically on the MPN clone. In conclusion, a chaperone, CALR, can turn into a rogue cytokine through somatic mutation of its encoding gene.

Introduction

Frameshifting (−1/+2) mutations in the exon 9 of the calreticulin (*CALR*) gene are responsible for 20% to 30% of cases of essential thrombocythemia (ET) and primary myelofibrosis (PMF).[1,2] Belonging to the *BCR-ABL*–negative myeloproliferative neoplasms (MPNs), ET and PMF are clonal malignancies of the hematopoietic system. The 2 major prevalent exon

9 frameshifting mutations of *CALR* are a 52–base-pair deletion (type 1: del52, c.1092_1143del) and a 5–base pair insertion (type 2: ins5, c.1154_1155insTTGTC).[1,2] The oncogenic mutant CALR protein has been shown to always result from a −1/+2 frameshifting mutation in the exon 9 of the *CALR* gene. This leads to a novel mutant C-terminal end tail that is rich in positively charged and hydrophobic residues, unlike the wild-type (WT) CALR,[3] and loses the endoplasmic reticulum (ER)–retention KDEL signal peptide.

We and others have shown that the mutant end tail of CALR enables the specific pathological activation of the thrombopoietin receptor (TpoR),[4-10] which, via the Janus kinase/signal transducers and activators of transcription (JAK-STAT) pathway, drives the proliferation of hematopoietic cells. Mutant CALR and TpoR complexes traffic through the secretory pathway to the cell surface.[11,12] CALR mutants require oligomerization in order to activate TpoR[12,13] and the first N-glycosylation site of TpoR at residue Asn117 to be present for oncogenic activation.[4] Asn117 remains immature *N*-glycosylated at the cell surface because CALR mutants shield it from processing in the Golgi apparatus.[12] CALR mutants were reported by others and us to be circulating in the peripheral blood of patients with *CALR*-mutated MPNs or of engineered mice.[14-17] WT CALR may also go to the cell surface under specific conditions,[11,18-21] or be secreted by macrophages to enhance phagocytosis of cancer cells.[22]

Here, we asked whether secreted mutant CALRs may act in a paracrine and/or autocrine fashion to activate the TpoR of adjacent cells and whether this "rogue cytokine" effect would be relevant to MPN pathogenesis.

Methods

ELISA

Enzyme-linked immunosorbent assay (ELISA) plates were coated with a polyclonal rabbit antibody (SAT602) or a monoclonal rat antibody (clone 11) that recognize a peptide derived from the mutant CALR C-terminal sequence. After blocking (5% bovine serum albumin [BSA] + 0.05% Tween-20 in phosphate-buffered saline), plates were probed with plasma samples diluted in blocking buffer. Purified mutant CALR protein produced in Expi-293F cells (Thermo Fisher Scientific, Merelbeke, Belgium) was included as a standard for quantification. For detection, an anti-CALR antibody (FMC75, Abcam, Cambridge, United Kingdom) in combination with an antimouse immunoglobulin G–HRP antibody (Southern Biotech, Birmingham, AL) was used and 3,3′,5,5′-tetramethylbenzidine (Thermo Fisher Scientific) was added as substrate. Absorbance was measured with a microplate reader (SpectraMax i3, Molecular Devices, Silicon Valley, CA) at 450 and 620 nm. For measuring stability of recombinant human CALR-del52 (rhCALR-del52), we incubated rhCALR-del52 in either indicated medium or plasma from a healthy individual for several periods at 37°C and then measured levels by ELISA, with detection with a chicken monoclonal antibody raised against the C-terminal mutated tail in combination with an antichicken immunoglobulin G–HRP antibody (Abcam, Cambridge, United Kingdom).

Transcriptional assays

Dual-luciferase assay was performed as previously described.[4]

Immunoelectron microscopy

Cells were fixed using 4% paraformaldehyde, 0.5% glutaraldehyde, and 1.4% sucrose (pH 7.4), then embedded in London Resin White according to manufacturer protocols (Agar Scientific, United Kingdom). Sections were labeled on grid with a primary antibody, then a gold-conjugated secondary antibody at 1:250 dilution (gold size: 0.8, 6, or 10 nm; Aurion, The Netherlands). Primary antibody was omitted for negative controls. Blocking was done with BSA (0.2%) and a solution for goat antibodies (Aurion, The Netherlands). Micrographs were recorded using the 4k × 4k Ceta camera of a Talos 200C transmission electron microscope (Thermo Fisher Scientific), at 22 000× to 36 000× nominal magnification.

Confocal microscopy

HEK293T cells were plated on ibidi µ-slides and transfected with TFR1-mCherry and CALR-linker–green fluorescent protein fusion proteins 48 hours before imaging. Live cells were examined with a confocal server spinning disk Zeiss platform equipped with a 100× objective.

MK colony-forming unit assay using human samples

$CD34^+$ cells were purified from patient peripheral blood and cultured for 3 days in serum-free medium in the presence of thrombopoietin (Tpo) (20 ng/mL) (Kirin Brewery, Tokyo, Japan) and stem cell factor (SCF) (25 ng/mL) (Biovitrum AB, Stockholm, Sweden). $CD34^+CD41^+$ progenitors were sorted using anti–CD34-fluorescein isothiocyanate and anti–CD41-phycoerythrin and were cloned at 1 cell per well in 96-well plates in serum-free medium without cytokine with SCF only, SCF + Tpo (20 ng/mL), SCF ± rhCALR WT, or SCF ± rhCALR-del52. Megakaryocyte (MK) colonies were counted at day 5.

Proliferation assay (CellTiter-Glo assay)

Proliferation assays were performed as previously described.[4]

NanoBRET assay and conditioned medium preparation

NanoBRET experiments were performed as previously described.[12]

Results

Mutant CALR proteins are detectable in the plasma of patients with MPN and correlate with the status of disease

A total of 159 plasma samples from patients were analyzed by ELISA for presence of circulating mutant CALR proteins using a specific antibody that does not recognize nonmutated CALR (111 *CALR* mutated, 35 *JAK2*-V617F positive, 2 triple negative, and 11 healthy controls). Soluble mutant CALR was detectable in 106 of 111 patients with mutated *CALR* with a mean level of 25.64 ng/mL. No signal was detected for patients who were *JAK2*-V617F positive or triple negative or for healthy controls (Figure 1A). The most represented CALR mutation was type 1–del52 (64 patients), followed by type 2–ins5 (33 patients). In addition, 14 less common mutations were observed (1 patient for each variant). Grouping all the mutations in type 1–like, type 2–like, and other mutations did not reveal any significant difference in the amount of soluble mutant CALR among the first 2

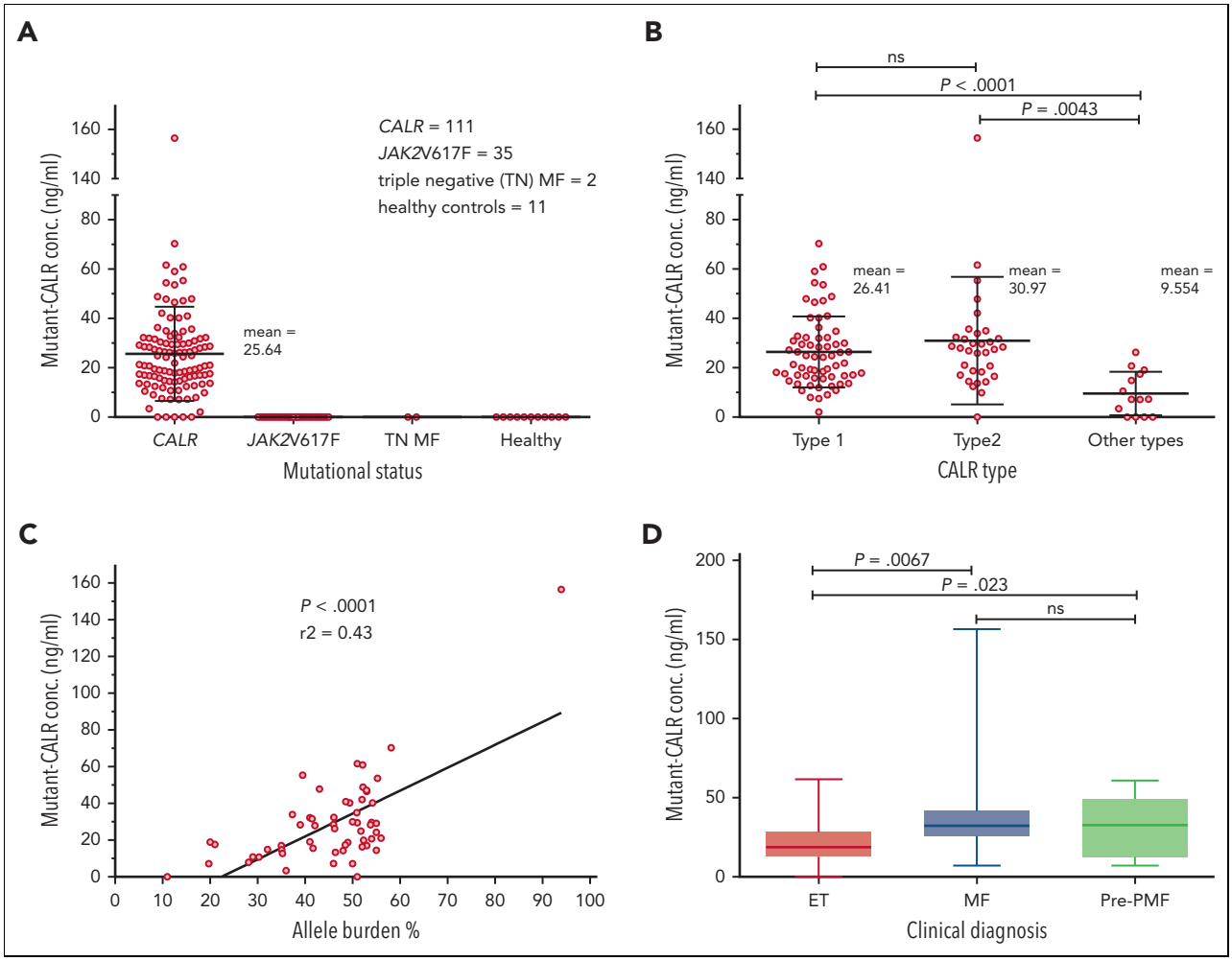

Figure 1. Quantification of mutant CALR in plasma from patients with MPN and correlation of protein levels to the disease state. (A) Quantification of free mutant CALR proteins in the plasma from patients with MPN, separated by their mutational status, and assayed by ELISA. Red bars represent mean ± standard deviation (SD). (B) The same ELISA results for patients with mutated *CALR* as shown in panel A, separated according to their mutation type. Red bars represent mean ± SD. (C) XY plot of the allele burden of each patient by their level of free plasmatic mutant CALR. A linear regression was applied and shows a statistically significant correlation between the 2 parameters. (D) The same ELISA results for patients with mutated *CALR* as shown in panel A, represented as a box and whisker plot, arranged according to patient disease status. All statistical analysis (using the Prism6 software) were performed by the unpaired *t* test. conc., concentration; MF, myelofibrosis; ns, not significant; TN, triple-negative.

groups but was significantly lower in patients carrying other types of mutations (Figure 1B). Interestingly, 4 of 5 samples with nondetectable mutant CALR belong to patients carrying uncommon mutation types, del22, del1, type28, and type34, as defined by Klampfl et al.[2] Mutational CALR burden and clinical diagnosis data were available for 57 patients. From those, plasma levels of soluble mutant CALR were directly correlated to the allele burdens in the blood (Figure 1C). We observed that soluble mutant CALR levels were significantly higher in patients with a diagnosis of PMF or pre-PMF when compared with patients with a diagnosis of ET (Figure 1D).

Immunoelectron microscopy detects mutant CALR proteins in the Golgi apparatus and secretory vesicles

The aforementioned results suggest that mutant CALRs are secreted by the MPN clone. We established the presence of mutant CALR in the secretory pathway of cells that also express TpoR,[12] and at the same time, we asked whether CALR mutants are also localized in the secretory pathway in cells that only express CALR mutants, like myeloid or lymphoid cells of the mutated *CALR* clone. To this end, we used transmission electron microscopy firstly on pro-B BaF3 cells expressing either CALR-del52 or CALR WT tagged with a flag sequence at the C-terminus in the absence of TpoR. Immunoelectron microscopy with antiflag and gold-conjugated secondary antibody showed that CALR-del52 localized in both the cis-Golgi and trans-Golgi compartments, as well as in various vesicles distributed between the trans-Golgi network and the plasma membrane (Figure 2A). CALR WT was mostly localized in the ER and to a lesser extent in the nucleus, with very low levels in the cis- or trans-Golgi (Figure 2B).

We then turned to clustered regularly interspaced short palindromic repeats -modified BaF3 TpoR *Calr*^{mut} cells that express endogenous levels of mutant CALR (described previously[10]). Using an anti–N-terminus CALR antibody, we noted plasma membrane labeling (Figure 2C), suggesting that secretion of mutant CALR is maintained in this cell line. In contrast, in control clustered regularly interspaced short palindromic repeats cells,

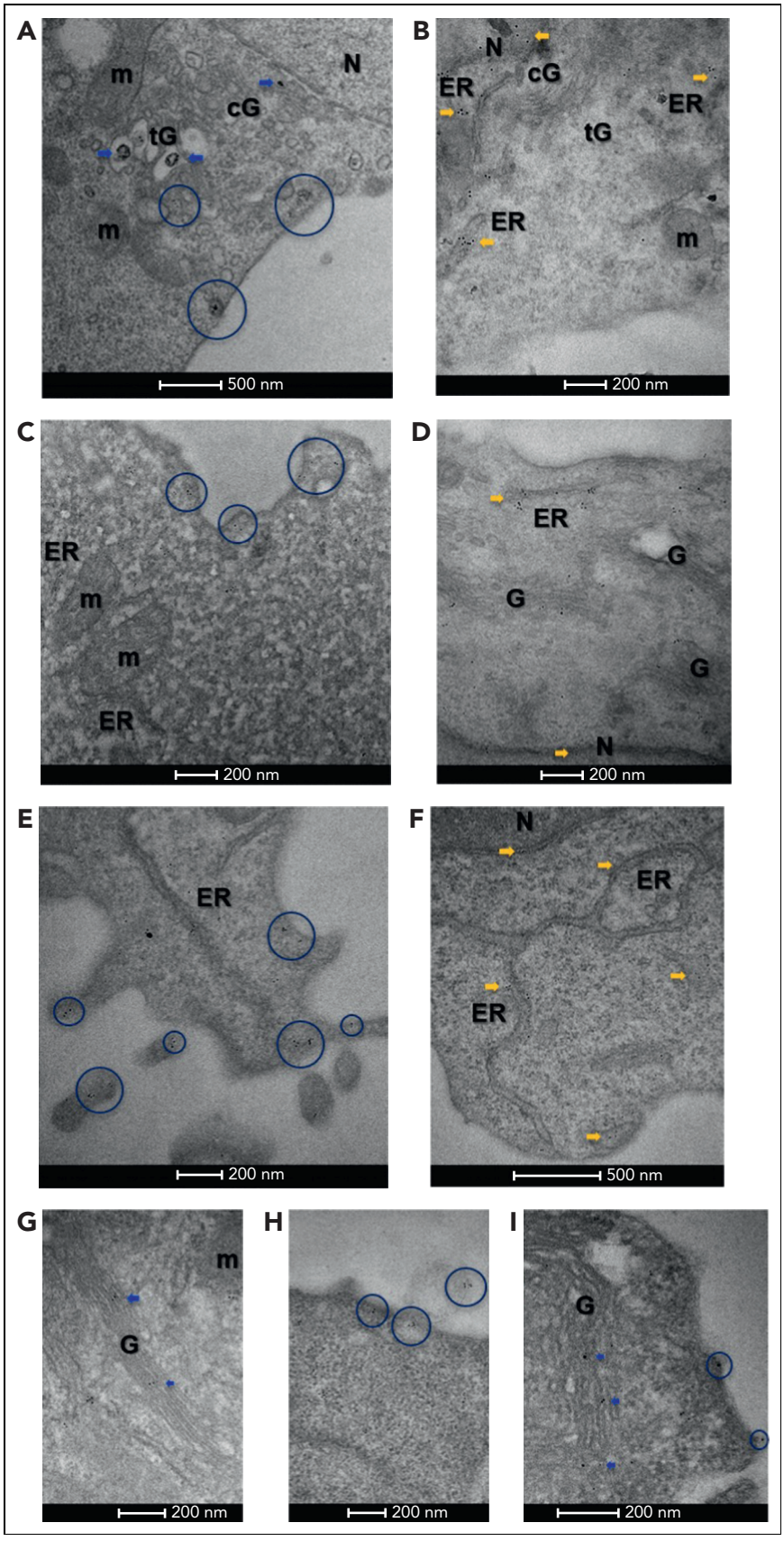

Figure 2. Immuno-electron microscopy of CALR. (A) In BaF3 cells, Flag-tagged CALR-del52 localized in both the cis-Golgi (cG) and trans-Golgi (tG) compartments (blue arrows), as well as vesicles distributed between the trans-Golgi network and the plasma membrane (blue circles), suggesting it follows the secretory pathway to the cell surface. (B) By contrast, Flag-tagged CALR WT predominantly localized in the ER and nuclear heterochromatin (yellow arrows) and was less frequent in the Golgi network (cG, tG). (C) In cytokine-independent, proliferating clustered regularly interspaced short palindromic repeats (CRISPR)-modified BaF3 TpoR *Calr*^{mut} cells, which expressed both CALR-del52 as well as endogenous CALR, anti–N-terminus labeling was frequently observed at the plasma membrane (blue circles), suggesting CALR secretion is maintained in this cell line. (D) In control CRISPR BaF3 TpoR *Calr*^{wt} cells, endogenous CALR localized mostly in the nucleus (N), perinuclear space, ER (yellow arrows), and the Golgi (G) network. (E) In primary *Calr* $^{del52/WT}$ KI mouse bone marrow cells, N-terminus–labeled CALR could be detected within the Golgi network (not shown), as well as at the plasma membrane (blue circles), suggesting secretion of CALR is maintained in these cells. (F) In control *Calr* $^{WT/WT}$ mouse bone marrow cells, endogenous CALR was mostly localized at the ER and the nucleus (N). When using a mutant-specific anti-CALR antibody labeling could be detected in the Golgi network of CRISPR-modified BaF3 TpoR *Calr*^{mut} cells (G) (blue arrows) but also at the plasma membrane (H), including associated with ectosomes (blue circles). (I) Similarly, the mutant-specific antibody identified CALR-del52 in the secretory pathway of *Calr* $^{del52/WT}$ KI mouse bone marrow cells (blue arrows and circles). Gold particle size is on average 0.8 nm in panel A and 6 or 10 nm in panels B to I. Scale bars represent 500 nm (A,F) and 200 nm (B-E,G-I). m, mitochondria.

endogenous WT CALR localized mostly in the ER and perinuclear space, nucleus, and weakly in the Golgi network (Figure 2D). Similar differences were observed in primary bone marrow cells from *Calr*$^{del52/WT}$ knockin (KI) mice and *Calr*$^{WT/WT}$ controls with an anti–N-terminus antibody (Figure 2E-F). Finally, we confirmed these data using a mutant CALR–specific antibody, SAT602, which detects the C-terminus of the mutant CALR-del52. The antibody also demonstrated labeling of plasma membrane and vesicles between trans-Golgi network and plasma membrane, as well as ectosomes, in the BaF3 TpoR *Calr*^{mut} cell line (Figure 2G-H) and primary bone marrow cells from *Calr* $^{del52/WT}$ KI mice (Figure 2I).

Next, we tested in vivo whether secretion occurs only from TpoR cells or also from other cells of the clone. We used *Calr*$^{del52/WT}$ KI mice that had been crossed with *Mpl*$^{-/-}$ mice. Remarkably, although intracellular CALR-del52 was strongly reduced in the absence of TpoR, it was still highly present in the plasma in mice lacking TpoR (Figure 3A). The high proportion of plasma CALR-del52 in *MPL*$^{-/-}$ mice despite low intracellular expression suggested that cells that do not express TpoR are more able to secrete it. Consistently, comparison of secretion levels in cells cotransfected with CALR-del52 and either TpoR or an empty vector revealed that the lack of TpoR resulted in enhanced secretion of CALR-del52 (supplemental Figure 1A, available on the *Blood* website). Flow cytometry analysis showed that cell surface CALR-del52 was also increased in absence of TpoR (supplemental Figure 1B). Together, this suggests that the main source of plasma mutant CALR comes from cells of the clone that do not express TpoR.

Plasma sTFR1 is a carrier protein for mutant CALR

To study the functional relevance of extracellular mutant CALR, we produced rhCALR-del52 and rhCALR WT (supplemental Figure 2A-B) and validated its correct folding by thermal shift (supplemental Figure 2C). We assessed the stability of rhCALR-del52 by measuring its half-life in culture medium (without serum supplementation) after incubation at 37°C and detection by ELISA. Analysis revealed a half-life of 30.72 minutes (Figure 3B). Strikingly, the stability of plasma mutant CALR was >10 times higher with an average half-life of 426.3 minutes (Figure 3C), and immunoprecipitation followed by western blotting confirmed that CALR proteins were intact (Figure 3D, left) and quantification validated the levels detected by ELISA (Figure 3D, right). To assess whether mutant CALR could be stabilized by other proteins in plasma, we immunoprecipitated the plasma from 5 patients and 5 healthy controls with a mutant C-terminus–specific antibody (Figure 4A-B) and analyzed the coprecipitating proteins by mass spectrometry. The plasma soluble ransferrin receptor 1 (sTFR1) was the only protein detected in large quantities in 5 out of 5 patients and not in control samples (Figure 4C; supplemental File 1). The presence of the sTFR1-mutant CALR complex in the plasma of 4 additional patients was confirmed by western blotting with anti-TFR1 antibody after immunoprecipitation of mutant CALR (supplemental Figure 3A). To estimate the fraction of plasma mutant CALR in complex with sTFR1, we quantified by western blotting the amount of sTFR1 that coimmunoprecipitated with plasma CALR from 4 other patients. By also measuring the amount of plasma mutant CALR in the immunoprecipitation product, we could approximate the fraction of plasma CALR in complex with sTFR1 to an average of ~60% for these 4 patients given a 1:1 molar ratio (supplemental Figure 3B-D).

These results suggested that sTFR1 could act as a carrier protein of plasma mutant CALR and increase its half-life. We measured the stability of rhCALR-del52 in the culture medium with 10% fetal bovine serum supplemented or not with 2 or 4 μg/mL sTFR1. The addition of serum resulted in a higher half-life (73.38 minutes) and a gradual increase in stability was observed with 2 μg/mL (113.3 minutes) and 4 μg/mL (143.2 minutes) of sTFR1, in the range of normal sTFR1 plasma concentration (~5 μg/mL[23]) (Figure 4D). Interestingly, like TpoR, TFR1 is a highly N-glycosylated protein. This led us to hypothesize that interaction between mutant CALR and TFR1 could already occur in the secretory pathway. We used confocal microscopy to assess intracellular colocalization between TFR1-mCherry and CALR–green fluorescent protein fusion proteins in living cells. CALR WT exhibited an ER-like localization without significant colocalization with TFR1, whereas CALR-del52 was mostly present in intracellular vesicles and strongly colocalized with TFR1 (Figure 4E). By mass spectrometry, we found that, like TpoR,[12] TFR1 retained a high proportion of high mannose immature N-glycans on Asn251 in cells expressing CALR-del52 (Figure 4F). Remarkably, this differential N-glycosylation was only detected in the cleaved fragment of TFR1 that is secreted, hinting that CALR-del52 might favor its cleavage, as also suggested by the increased cleaved fraction in CALR-del52–expressing cells (Figure 4F). We concluded that stabilization of the complex is favored by the N-glycans interactions formed intracellularly and that adding mutant CALR to plasma will not recover all interactions, as the recombinant sTFR1 possesses fewer immature sugars than the one secreted with mutant CALR.[24] This explains why adding CALR-del52 to plasma from healthy controls only very modestly increased the half-life from 30 to 45 minutes (supplemental Figure 2D).

Mutant CALR proteins initiate proliferation of BaF3 cells expressing TpoR and mutant CALR in a rogue cytokine fashion

To probe the ability of soluble CALR to induce cytokine-independent proliferation of BaF3 cells, we first defined the amount of recombinant CALR that best mimicked plasma levels of mutant CALR found in patient plasma. We referred to basic pharmacokinetic equations to derive the single-dose concentration that would best mimic an average steady state concentration similar to what is observed in vivo. The average plasma concentration (C_p) is given by Rowland and Tozer:[25] $C_p = \frac{1}{0.693} \times F \times D \times t_{\frac{1}{2}} \times \frac{1}{\tau}$ In which F is the bioavailability, D is the dose, $t_{1/2}$ is the half-life, and τ is the dose interval.

The bioavailability was assumed to be maximum in vitro so that F = 1, half-life was determined experimentally in culture medium with 10% fetal bovine serum (Figure 4D), and the dose interval was set at τ = 24 hours. Supplemental Table 1 gives the relationship between single-dose treatment and corresponding average plasma concentration (C_p) over the experimental time frame. In comparison, recombinant truncated human Tpo used in in vitro assays is similar to that described by Thomas et al[26] with a half-life of 1.56 hours. A single dose of recombinant truncated human Tpo of 10 ng/mL over 24 hours thus has an average plasma concentration C_p of 0.94 ng/mL, slightly

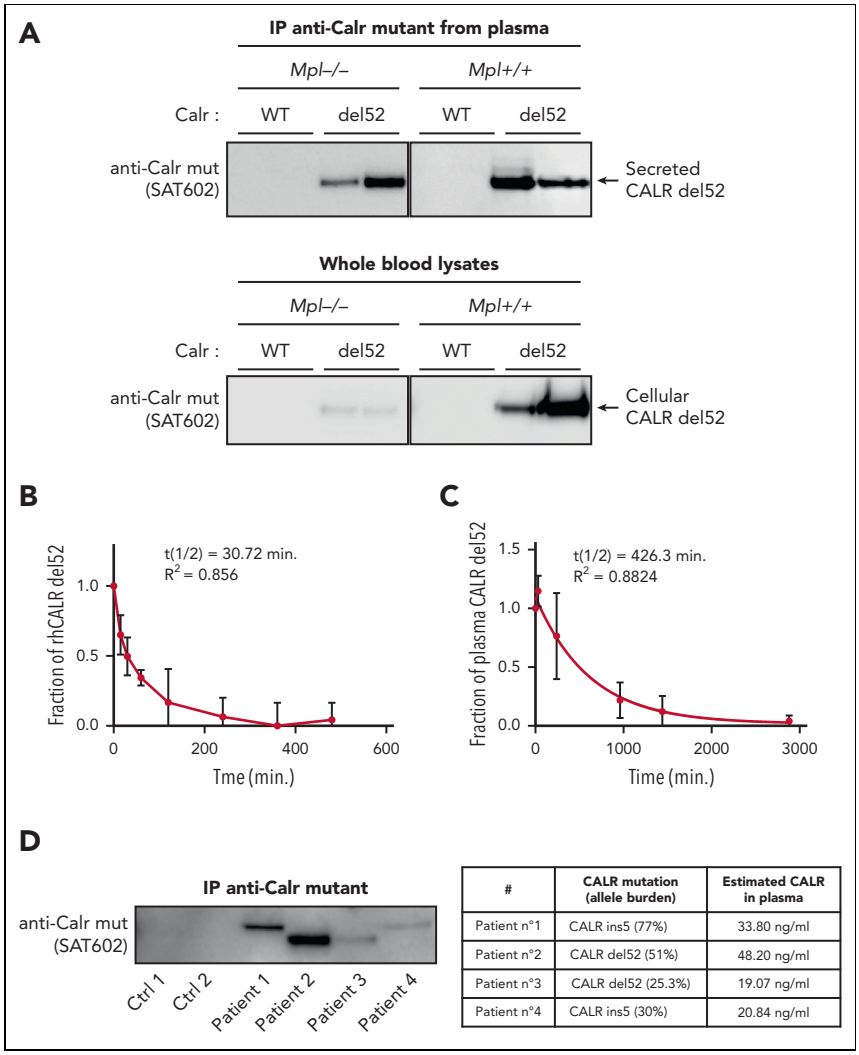

#	CALR mutation (allele burden)	Estimated CALR in plasma
Patient n°1	CALR ins5 (77%)	33.80 ng/ml
Patient n°2	CALR del52 (51%)	48.20 ng/ml
Patient n°3	CALR del52 (25.3%)	19.07 ng/ml
Patient n°4	CALR ins5 (30%)	20.84 ng/ml

Figure 3. Secretion and stability of plasma CALR-del52 from Calr-del52/WT KI mouse and patients with MPN. (A) Immunoprecipitation (IP) of murine plasma CALR-del52 and whole-blood lysates. Secretion rate of CALR-del52 was evaluated by comparing the cellular and plasmatic CALR-del52 levels from blood of KI-*Calr* $^{del52/WT}$ mice expressing or not expressing TpoR. (B) Stability study of mutant CALR in plasma from patients with MPN harboring mutated CALR-del52. Samples (n = 8) from patients with MPN harboring mutated CALR-del52 maintained at 37°C for various time points were measured in duplicate by ELISA and analyzed using a 1-phase decay model (Prism6) to determine the averaged half-life (t½) and the coefficient of determination (R^2). Error bars represent SDs. (C) Stability study of rhCALR-del52 in culture medium in absence of fetal bovine serum. A fixed amount of rhCALR-del52 was incubated in culture medium at 37°C for various lengths of time before measurement by ELISA analysis using a 1-phase decay model (Prism6) to determine the averaged half-life and R^2. Error bars represent SDs. (D) CALR mutant proteins after immunoprecipitation in various MPN patients (left) and CALR mutant proteins quantification by western blotting (optical density) of the same patients (right). Ctrl, control; mut, mutant.

above the range of plasma Tpo detected in healthy controls (0.108-0.506 ng/mL).[27]

Based on the aforementioned results, we used several concentrations of CALR-del52 from 0.01 µg/mL (C_p = 0.73 ng/mL) to 100 µg/mL (C_p = 7.3 µg/mL) with a dosing interval of 24 hours. Using this approach, we measured proliferation of BaF3 cells at 72 hours. Remarkably, we could already detect a significant increase at 0.01 µg/mL (C_p = 0.73 ng/mL) and a dose-dependent increase up to 100 µg/mL (C_p = 7.3 µg/mL) (Figure 5A) in BaF3 TpoR *Calr*$^{mut\ 10}$ cells but not in BaF3 parental or BaF3 TpoR *Calr*^{WT} cells that do not express mutant CALR. Cells that coexpress TpoR and mutant CALR are thus hypersensitive to exogenous mutant CALR proteins compared with cells that only express WT endogenous CALR. In comparison, the addition of 10 ng/mL Tpo resulted in increased proliferation, similar to that induced by an average plasma concentration of C_p 73 ng/mL, in the range of what was found in patients' plasma (Figure 5B). A 50% effective dose was estimated at ~100 ng/mL of rhCALR-del52 on the growth of BaF3 TpoR *Calr*^{mut} cells, in the range of plasma concentrations found in patients. In comparison, the Tpo 50% effective dose was 0.62 and 2.02 ng/mL in BaF3 TpoR *Calr*^{WT} and BaF3 TpoR *Calr*^{mut} cells, respectively. Remarkably, maximum response was higher with exogenous CALR-del52 than with Tpo for BaF3 TpoR *Calr*^{mut} cells, indicating that the latter respond better to plasma mutant CALR than to Tpo (supplemental Figure 4). The ability of rhCALR-del52 to induce proliferation BaF3 TpoR *Calr*^{mut} cells was further confirmed by thymidine incorporation experiment (supplemental Figure 5A).

Low levels of soluble CALR mutants are able to induce JAK-STAT signaling by selectively activating TpoR at the cell surface of *Calr*-mutated cells

To measure the activation of the JAK-STAT pathway specifically, we transfected the Spi-Luc luciferase STAT5 reporter[28] in BaF3 TpoR *Calr*^{mut}, BaF3 TpoR *Calr*^{WT}, or parental BaF3 cells and measured STAT5 activation 24 hours after stimulation with rhCALR-del52. In BaF3 TpoR *Calr*^{mut} cells we could detect a dose-dependent STAT5 activation by rhCALR-del52 starting at 0.1 µg/mL (C_p = 7.3 ng/mL) (twofold) and a plateau (fourfold) achieved at 1 µg/mL (C_p = 73 ng/mL), as compared with vehicle (Figure 5C). Like for the growth assay, the activity induced by 1 µg/mL (C_p = 73 ng/mL) of rhCALR-del52 was comparable with stimulation by 10 ng/mL of Tpo (C_p = 0.94 ng/mL).

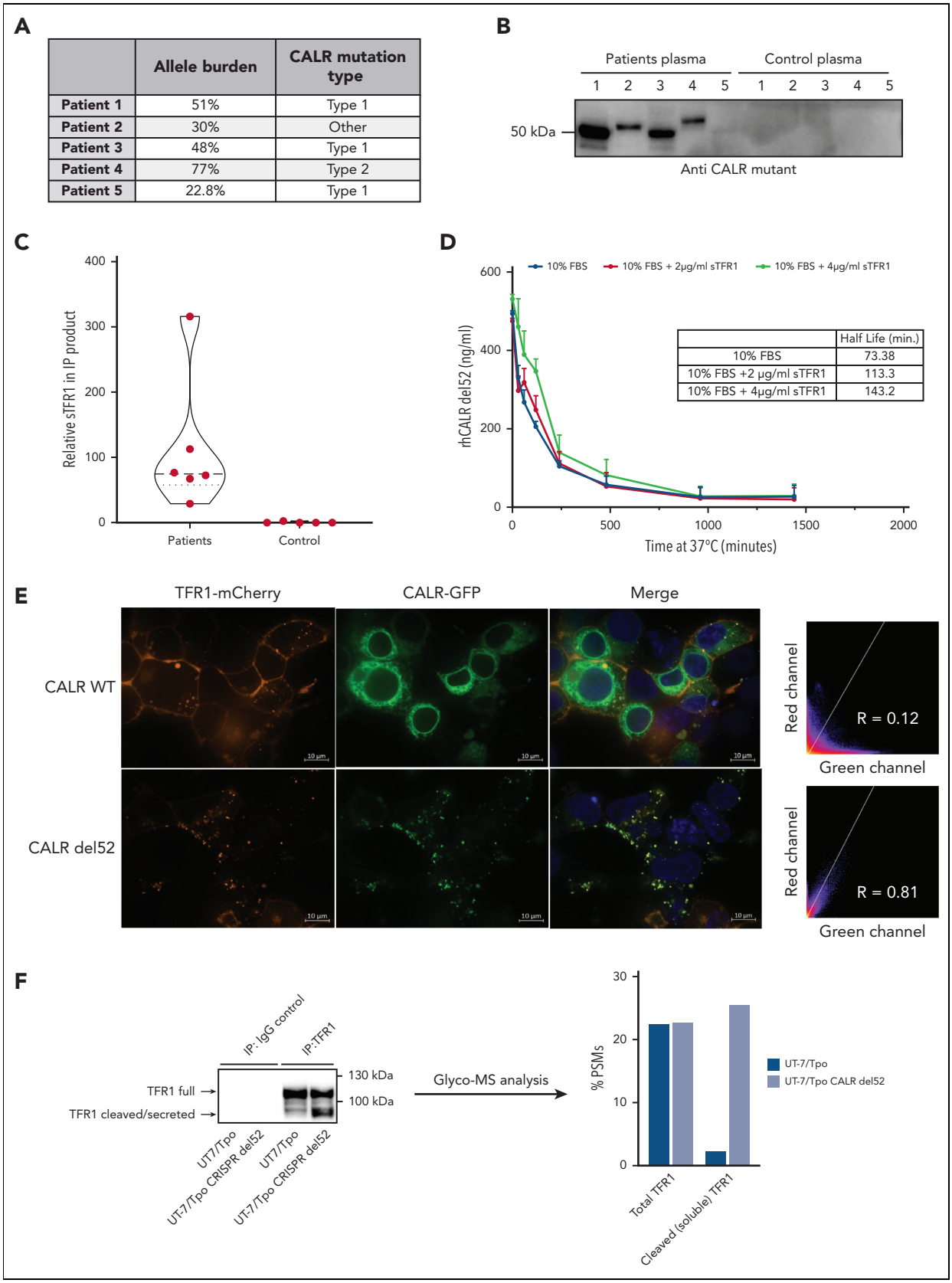

Figure 4. sTFR1 is a carrier protein for mutant CALR. (A) Allele burden and mutation profile of patients included in this study the analysis. (B) Identification of partners of plasmatic mutant CALR. Plasma from 5 patients with mutated CALR and 5 healthy controls was isolated by IP with biotinylated antimutant CALR antibody. Immunoblot shows the presence of mutant CALR in the IP product detected with a different antimutant CALR antibody. The IP product was analyzed by nontargeted MS to identify interacting partners. (C) Truncated violin plot of relative sTFR1 amount found coimmunoprecipitating with plasma CALR-del52. Negative control corresponds to the IP product after

In sharp contrast, BaF3 TpoR *Calr*^{WT} cells required a considerably higher concentration of rhCALR-del52 (100 μg/mL, C_p = 7.3 μg/mL) in order to detect a 2.5-fold increased STAT5 activation, thus a 1000-fold difference in sensitivity (supplemental Figure 5B), and parental BaF3 cells were not stimulated by rhCALR-del52 (supplemental Figure 5C). Surprisingly, we could detect a 1.5- to twofold increased STAT5 activation upon stimulation of BaF3 TpoR *Calr*^{mut} cells with 10 to 100 μg/mL of rhCALR WT, respectively, thus a 100- to 1000-fold difference when compared with rhCALR-del52 (Figure 5C). CALR WT could be interacting with surface-bound TpoR-mutant CALR complexes and stabilizing them, possibly pointing to a potential low intrinsic affinity of CALR globular domain for TpoR.

We then verified that TFR1 did not prevent mutant CALR–mediated activation of TpoR. Because interaction of mutant CALR with TFR1 relies, at least partially, on interaction with immature N-glycans (Figure 4F), we first used the approach of intracellular TFR1 overexpression. Overexpression of TFR1 did not prevent but rather promoted CALR-del52–induced proliferation of UT-7/Tpo CALR-del52 but not UT-7/Tpo control cells[29] (supplemental Figure 5D). Likewise, addition of recombinant exogenous sTFR1, which retains immature glycans on Asn727, but not on Asn251,[24] to the culture medium did not prevent but increased activation of TpoR by CALR-del52 in a rogue cytokine fashion (Figure 5D)

Next, we confirmed the activation of the JAK-STAT pathway by detection of phosphorylated STAT5, extracellular signal-regulated kinase 1/2, and phosphorylated tyrosine 626 of the intracellular domain of TpoR,[30] in BaF3 TpoR *Calr*^{mut} cells poststimulation by 0.1 μg/mL (C_p = 7.3 ng/mL) for several time points (Figure 5E). BaF3 parental cells did not show any such response up to 100 μg/mL (C_p = 7.3 μg/mL) rhCALR-del52 concentration (supplemental Figure 6A). Finally, we harvested megakaryocytic (CD41$^+$) cells harboring a heterozygous *Calr*-del52 mutation from the bone marrow of *Calr* $^{del52/WT}$ KI mice[14] (supplemental Figure 6B) and subjected the cells to western blotting after stimulation for 30 minutes with rhCALR-del52 or the vehicle control (supplemental Figure 6C). Upon stimulation with 10 μg/mL (C_p = 730 ng/mL) of rhCALR-del52, we detected an increased phospho-STAT5 signal when compared with the vehicle condition, showing that exogenous mutant CALR proteins effectively activate the TpoR of primary *Calr*$^{del52/WT}$ cells.

Soluble mutant CALR proteins can directly interact with TpoR at the cell surface

In a previous study, we provided evidence that when mutant CALR and TpoR are coexpressed in the same cell, a direct cis interaction can be documented either by bioluminescence resonance energy transfer or by size-exclusion chromatography.[12] We used our previously published NanoBRET constructs[12] and set up a cell coculture system assay to assess trans interaction between cells stably expressing either CALR-del52-HaloTag or NanoLuc-TpoR (NL-TpoR) (Figure 6A). Both construct types were properly expressed and/or secreted in the culture medium and recapitulated the signaling properties of the original protein (supplemental Figure 7). By coculture of these cells, we observed that CALR-del52-HaloTag has a stronger interaction with NL-TpoR in trans than that of CALR WT-HaloTag (Figure 6B). To confirm this finding, we incubated BaF3 TpoR CALR^{WT} or BaF3 TpoR CALR^{mut} cells with rhCALR-del52 for a short time frame (15 minutes) and measured by western blotting the binding of exogenous rhCALR-del52 to these cells after extensive washing (Figure 6C). Strongest binding was observed on BaF3 TpoR CALR^{mut} cells even at low physiological concentration (0.1 μg/mL) (Figure 6D). At higher concentration (0.5 μg/mL), weak binding was also detected for BaF3 TpoR CALR^{WT} cells (Figure 6D), in line with our functional assays showing that much higher levels of rhCALR-del52 are required for activation of signaling in cells expressing TpoR and CALR WT but not the mutant CALR (supplemental Figure 5B).

Recombinant CALR-del52 can enhance the differentiation of human MK progenitors ex vivo

Next, we sought to validate the cytokine effect of rhCALR-del52 in primary cells from patients with MPN carrying *CALR* mutations or *JAK2* V617F or from healthy controls. We isolated CD34$^+$CD41$^+$ cells and performed MK colony assays in the absence or presence of rhCALR-del52 in medium containing KIT ligand (SCF) and lipids, insulin transferrin, and BSA. In this medium for colony assays, the half-life of rhCALR-del52 is ~35 minutes (Figure 7A).

First, we used a single dose of 20 μg/mL (C_p =120 ng/mL over 5 days) rhCALR-del52 and observed that rhCALR-del52 significantly increased the number of MK colonies, whereas CALR WT did not (Figure 7B). Importantly, rhCALR-del52 did not increase the number of MK colonies for patients with JAK2 V617F or for healthy controls (Figure 7C-D). Alternatively, we added a lower amount of rhCALR-del52 daily to mimic in vivo conditions in which CALR-del52 is continuously produced and to partially compensate the rapid disappearance of the recombinant protein. To this end, we added either 0.1 μg/mL (C_p = 3 ng/mL), 1 μg/mL (C_p = 30 ng/mL), or 5 μg/mL (C_p = 150 ng/mL) daily for 4 days. We could detect a significant increase in Tpo-independent MK colonies in the condition of 5 μg/mL (C_p = 150 ng/mL) rhCALR-del52 and a trend in the condition of 1 μg/mL (C_p = 30 ng/mL) (Figure 6E). Taken together, our data indicate that at levels comparable to the levels detected in patients, rhCALR-del52 induces a significant increase in MK colony formation.

Figure 4 (continued) anti–mutant CALR IP to control for nonspecific binding to anti–mutant CALR antibody. (D) Stability study of rhCALR-del52 in medium with 10% fetal bovine serum (FBS), with or without addition of 2 or 4 μg/mL of rhTFRC. rhCALR-del52 mutant in different media was maintained at 37°C for various lengths of time and measured by ELISA before analysis using a 1-phase decay model (Prism6) to determine the averaged half-life. Values represent mean of triplicate ± SD. (E) Representative confocal microscopy pictures of HEK293T cotransfected with either CALR WT or CALR-del52 fused to green fluorescent protein at the C-terminus and TFR1 fused to mCherry at its C-terminus. Scale bars represent 10 μm. Microscopy analysis shows colocalization between CALR-del52 and TFR1 in subcellular compartments with high correlation between the 2 constructs. (F) IP and glycosylation profile analysis of endogenous TFR1 from UT-7/Tpo or UT-7/Tpo CRISPR CALR-del52. Western blot shows the TFR1 forms analyzed by MS. Data represent the percentage of peptide-spectrum match of immature N-glycans (high mannose) present on residue Asn251 in the cleaved or full form of TFR1.

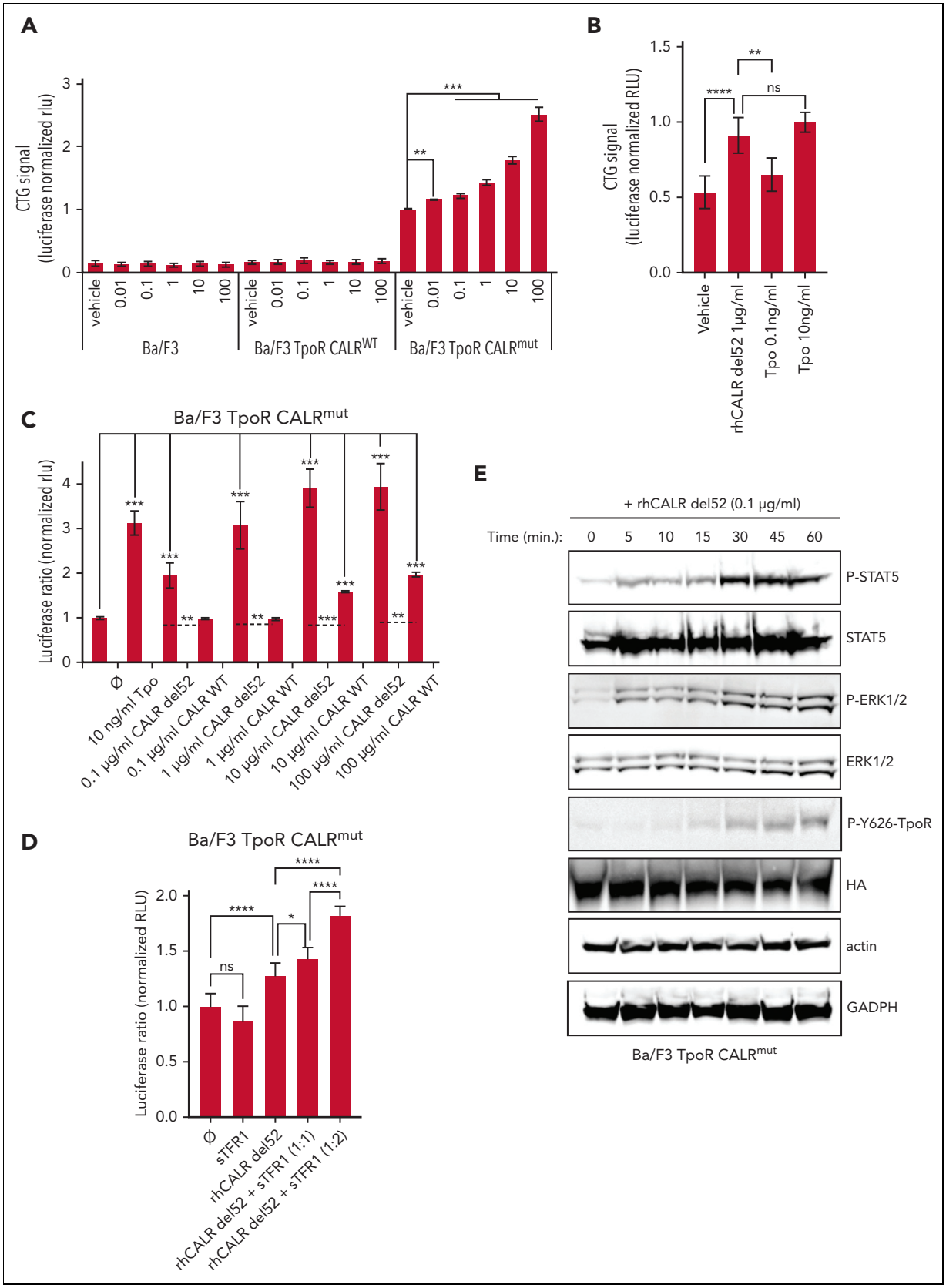

Figure 5. Exogenous CALR-del52 is inducing cell growth and JAK/STAT signaling in BaF3 cells expressing TpoR and mutant CALR. (A) Short-term proliferation of parental BaF3 and stable BaF3 cells expressing the indicated constructs were analyzed after daily exposition of the indicated doses of rhCALR-del52 over 72 hours with CTG assay (Promega). Values shown represent the average of 5 experiments with at least 29 biological replicates ± standard error of the mean (SEM). (B) Short-term proliferation of BaF3 TpoR CALR^{mut} cells was analyzed after daily exposition of 1 µg/mL of rhCALR-del52, 0.1 ng/mL of Tpo, or 10 ng/mL of Tpo over 72 hours with CTG assay (Promega).

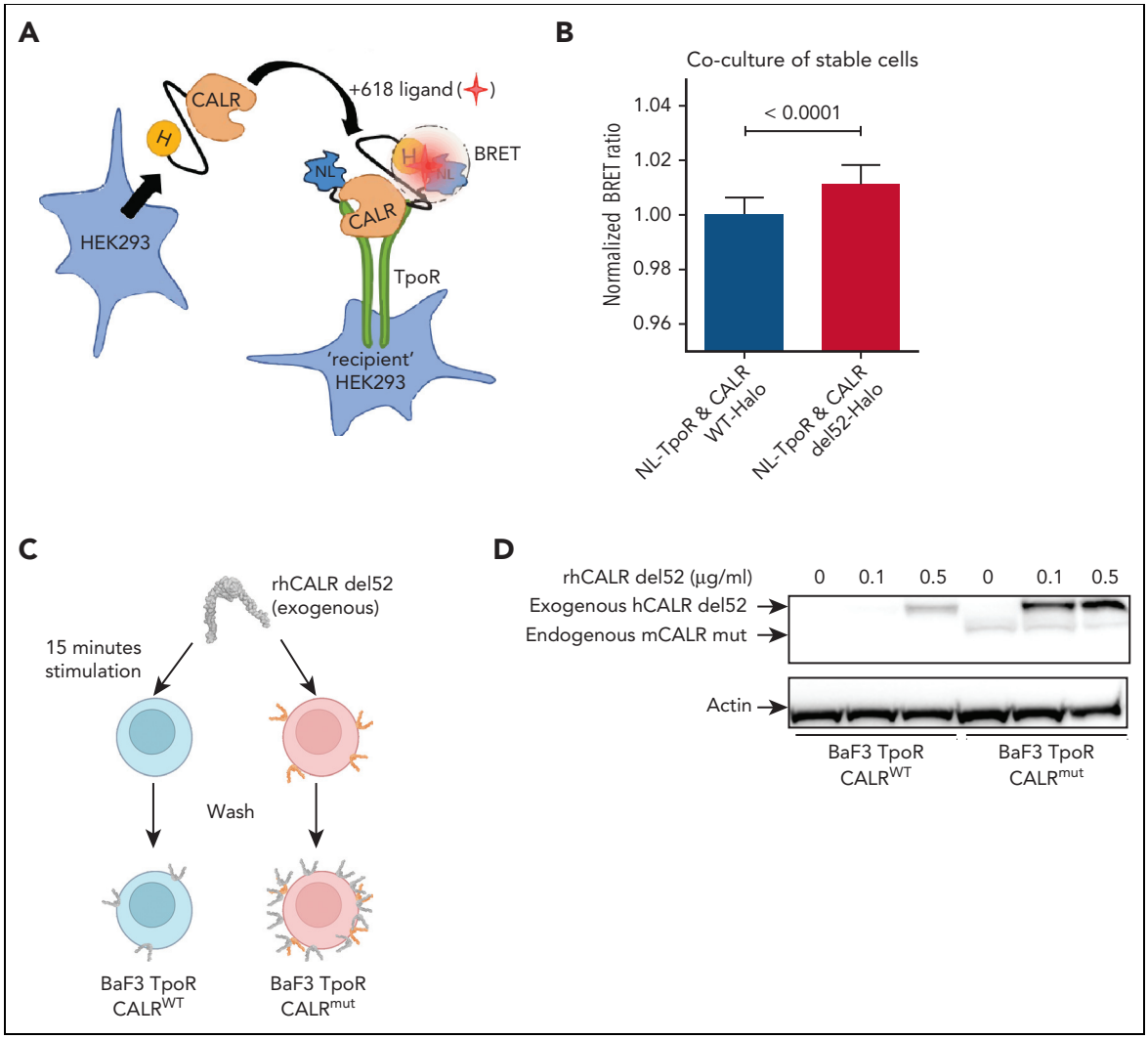

Figure 6. Binding of soluble mutant CALR proteins to TpoR at the cell surface. (A) Cartoon representation of our exogenous CALR, cell coculture NanoBRET setup. HaloTag (H) is fused to the C-terminal of CALR, nano-luciferase (NL) is fused to the N-terminal of TpoR, and 618-ligand is a fluorescent molecule with very high affinity for HaloTag. The circle represents a bioluminescence resonance energy transfer (BRET) phenomenon that occurs only when the energy donor (NL) is within 10 nm of the energy acceptor (618-ligand). (B) BRET detection between CALR-HaloTag and cell-surface nano-luciferase-TpoR in a stable cell coculture assay. HEK293 cells stably expressing either CALR WT or del52-HaloTag were cocultivated overnight in presence of 618-ligand with HEK293 cells stably expressing NL-TpoR. Data from 3 independent experiments were pooled and values were normalized to the NL-TpoR and CALR WT-Halo condition. Statistical analysis (Jmp pro14) was performed by a 2-tailed student *t* test and aforementioned *P* values. (C) Cartoon representation of our assay to measure binding of rhCALR-del52 to BaF3 TpoR *Calr*^{WT} and BaF3 TpoR *Calr*^{mut} cells. Cells were incubated for 15 minutes with varying amounts of rhCALR-del52 before extensive washing. (D) Western blotting showing the presence of rhCALR-del52 bound to BaF3 TpoR *Calr*^{WT} and BaF3 TpoR *Calr*^{mut} cells after 15 minutes incubation with different concentration of rhCALR-del52.

Discussion

Here, we show that patients with MPN who harbor *CALR* driver mutations exhibit plasma levels of mutant CALR proteins that correlate with the mutated *CALR* allele burdens. This finding raises the possibility of using the level of circulating mutant CALR proteins as a biomarker and risk stratification of *CALR*-mutated MPNs. Indeed, the mean levels of circulating CALR mutants significantly differ between patients with ET and those with (pre-)MF. Such secreted mutant CALR proteins can act as rogue cytokines to activate TpoR/JAK-STAT signaling in cell

Figure 5 (continued) Average ± SD of 6 replicates. (A-B). Statistical analysis (Jmp pro14) was performed by the nonparametric multiple comparisons Steel test with a control group (vehicle). ****$P < .0001$, ***$P < .001$, **$P < .01$. (C) BaF3 TpoR *Calr*^{mut} cells were transiently transfected with the Spi-Luc luciferase STAT5 reporter and the internal control pRL-TK used for normalization. The cells were cultured with different concentrations of recombinant human CALR-del52 or CALR WT over 24 hours before performing a Dual-Luciferase assay (Promega) for STAT5 transcriptional activity. (D) BaF3 TpoR *Calr*^{mut} cells transfected with Spi-Luc and pRL-TK were treated for 24 hours with vehicle or 1 µg/mL of rhCALR-del52 and indicated molar rations of rhTFRC and STAT5 transcriptional activity was measured by Dual-Luciferase assay. (C-D) Luciferase activity was normalized to vehicle condition (ø). Values shown represent the average of 6 to 12 biological replicates ± SEM. Statistical analysis (Jmp pro14) was performed by the nonparametric multiple comparisons Steel test with a control group (ø). ***$P < .001$, **$P < .01$, *$P < .05$. Statistical analysis of 2 specific conditions (see dashed lines) were performed by the unpaired *t* test. (E) Western blots showing time-dependent phosphorylation of TpoR, STAT5, and extracellular signal-regulated kinase 1/2 (ERK1/2) in BaF3 TpoR *Calr*^{mut} cells treated or not treated with 0.1 µg/mL rhCALR-del52 for various lengths of time (5, 10, 15, 30, 45, and 60 minutes). P-Y626-TpoR denotes phosphorylation of tyrosine residue 112 of the intracellular chain of TpoR. HA denotes detection of total HA-tagged TpoR. GAPDH, glyceraldehyde-3-phosphate dehydrogenase; HA, hemagglutinin (tag).

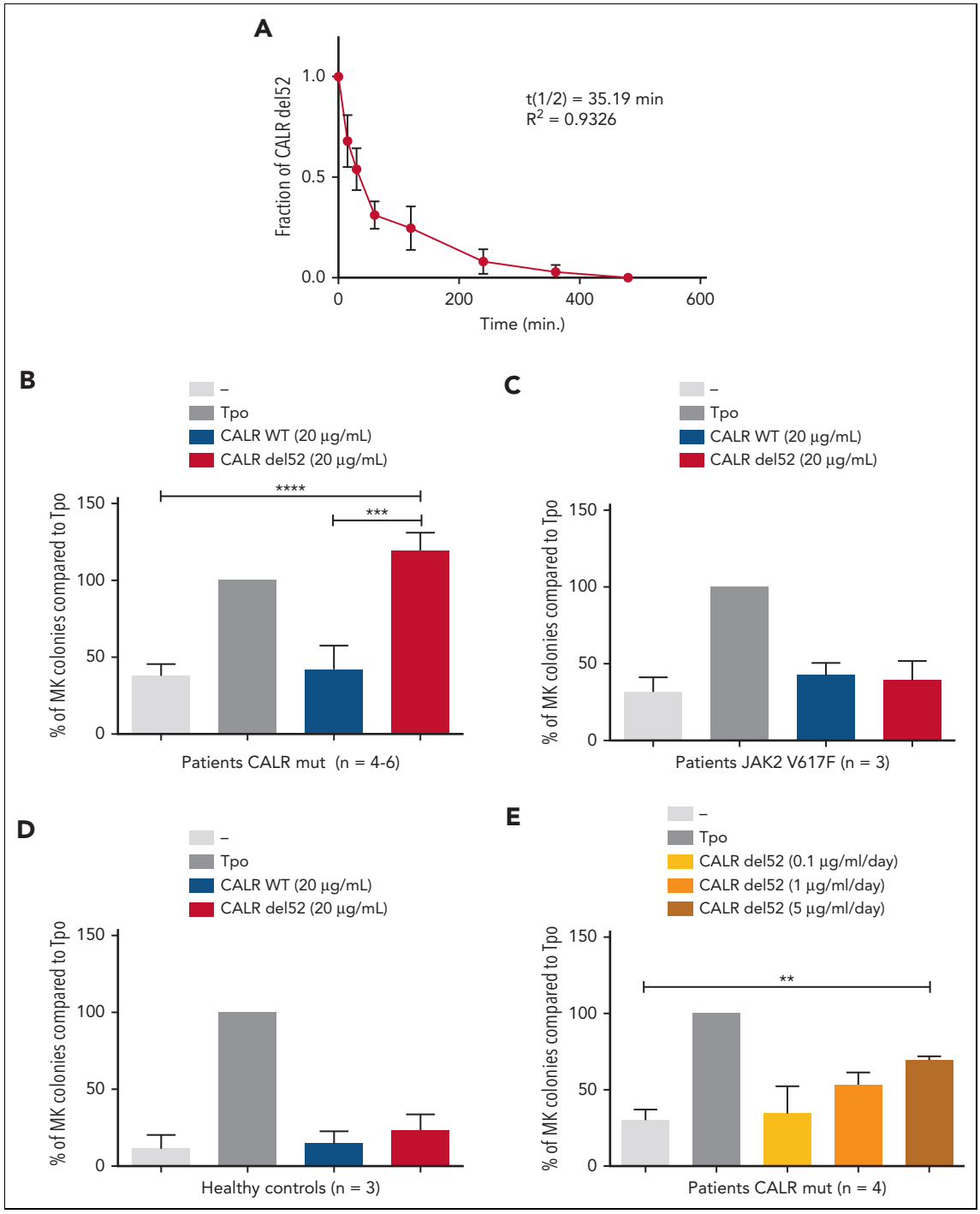

Figure 7. Induction of differentiation of MK progenitors by CALR-del52. (A) Stability study of rhCALR-del52 colony-forming unit MK culture medium. Six samples maintained at 37°C for various lengths of time were measured in duplicate by ELISA and analyzed using a 1-phase decay model (Prism6) to determine the averaged half-life and R^2. Error bars represent SDs. $CD34^+CD41^+$ progenitors from 4 to 6 patients with mutated CALR (B), 3 patients with JAK2 V617F (B), and 3 normal controls (C) were sorted and cloned at 1 cell per well in 96-well plates in serum-free medium containing SCF and treated with a single, large dose of CALR-del52. Percentages of MK colonies were calculated compared with the Tpo condition. Results are shown as mean ± SEM. ****$P < .0001$, ***$P < .001$. One-way analysis of variance, Holm-Sidak multiple comparisons test. (D) Effect of daily treatment of CALR-del52 (0.1, 1, or 5 µg/mL) on MK colony formation. $CD34^+CD41^+$ progenitors from 4 patients with mutated CALR were tested and the percentages of MK colonies were calculated compared with the Tpo condition. Results are shown as mean ± SEM. **$P < .01$. One-way analysis of variance, Holm-Sidak multiple comparisons test.

lines and patient primary cells. To our knowledge, this work is the first to demonstrate that circulating mutant CALR proteins can exert a rogue cytokine activity on cells that express the TpoR. Cells that carry an oncogenic mutation of *CALR* are more sensitive to levels of exogenous mutant CALR proteins similar to those detected in patient plasma. This can be explained by the observation that only cells expressing endogenous mutant CALR will expose at the cell-surface TpoR with immature (high

mannose) N-glycosylation[12] required for binding to the lectin domain of CALR.[31,32] We propose a model where mutant CALR proteins are secreted from *CALR*-mutated cells, including cells from the clone that do not express TpoR, and can enhance the activation of the TpoR of a nearby *CALR*-mutated cell in a paracrine fashion. This model would apply notably to the bone marrow niche were levels can be higher than in plasma. Although our work did not address the relative contribution of plasma vs intracellular mutant CALR for the expansion of the clone, our data indicate that plasma mutant CALR can act as an additional factor, reinforcing the constitutive activation of TpoR mediated by intracellular mutant CALR.[4-10]

The difference in half-lives between plasma CALR mutants and recombinant mutant CALR proteins in human plasma or culture medium indicates that upon secretion the mutant CALR proteins are in complexes with other proteins that stabilize them. We identified sTFR1 as a major partner that increases the half-life of mutant CALR proteins without preventing its rogue cytokine activity. Like TpoR, sTFR1 retained immature N-glycans specifically in the presence of mutant CALR, indicating that the interaction occurs intracellularly and that the relevant complex is the one secreted by cells. The identification of this novel interaction comes together with recent observations that iron metabolism is dysregulated in CALR-del52–expressing cells.[33] This suggests that this novel interaction might have broader effects on the pathology of MPNs beyond the stabilization of plasma mutant CALR.

Recently, levels of secreted CALR (WT and mutant) were assessed in KI models[14,17,34] and plasma from patients with MPN,[16] and are in agreement to ours. Remarkably, such secreted CALR had profound consequences on the immune response.[16] Our data suggest that removing the circulating mutant CALR proteins could affect the phenotype of the MPN disease. In fact, after in vivo injection of an antibody targeting mutant CALR, the detection and removal of circulating mutant CALR and the reduction of platelet numbers was achieved in a mouse model of MPN represented by KI of a chimeric murine-human CALR-del52, in which the tail of CALR-del52 was from the human sequence.[34]

Our finding that mutant CALR proteins act as rogue cytokines could open new perspectives for treating patients with *CALR*-mutated MPNs.

Acknowledgments

The authors thank Didier Colau for protein production and purification and guidance with respect to recombinant protein usage, Lidvine Genet for expert technical support, and Nicolas Dauguet for flow cytometry assistance.

This work was supported by fellowships from the de Duve Institute Morange Funds postdoctoral fellowship (A.R.) and by the FRS-FNRS fellowship (A.R.); a PhD Télévie fellowship (T.B.); an FSR PhD Fellowship from Université Catholique de Louvain (N.P.) and an Aspirant PhD Fellowship (N.P.) from the FRS-FNRS, Belgium. S.N.C. is Honorary Research Director at FRS-FNRS Belgium. This work was funded by the Ludwig Institute for Cancer Research, La Fondation contre le Cancer, Salus Sanguinis Fondation and Fondation "Les Avions de Sébastien," projets Action de recherché concertée 16/21 to 073, Projet de recherche FNRS number T.0043.21, and WelBio F 44/8/5-MCF/UIG-10955 (S.N.C.). The study was funded by grants from the Austrian Science Fund (P34451-B) and the Österreichische Forschungsförderungsgesellschaft (R.K.). Studies conducted at the University of Pavia were supported by a grant from Associazione Italiana per la Ricerca sul Cancro (MYNERVA project #21267) (M.C.). This work was funded by the Ligue Nationale contre le Cancer (équipe labellisée 2019) (V.W., I.P., A.T., M.E.-K., and C.M.), INCA PLBIO 2016 and 2021 (I.P.), and from the INSERM. Labex GR-Ex (I.P. and W.V.) is funded by the program "Investissements d'avenir." This work was supported by the university Paris-Diderot (MENRT grant) (A.T.) and the La ligue Nationale contre le cancer. This work was supported by a grant from the Romanian Ministry of Education Research and Innovation (grant number PN 19.29.01.02/2019) (T.E.F. and D.S.M.).

Authorship

Contribution: C.P., N.P., T.B., I. Chachoua, and A.T. planned paper strategy, performed experiments, interpreted data, and wrote the paper; C.P., A.N., I. Chachoua, G.V., and J.-P.D. planned and performed transcriptional experiments; C.P. performed functional murine cell lines and primary cell experiments; T.B. planned and performed bioluminescence resonance energy transfer experiments; N.P. performed mutant calreticulin (CALR) protein characterization from patient and primary mouse model plasmas and identified and characterized the transferrin receptor–CALR interaction in patient plasma; D.V. and N.P. performed MS experiments and analyzed the data; E.H., E.X., O.Z., R.K., H.N., and A.M. performed study on patient plasma; T.E.F., D.S.M., and A.R. performed immunoelectron microscopy; H.G., B.G., M.S., I. Casetti, E.R., D.P., C.C., L.A., M.C., N.K., Y.K., Y.S., Y.E., M.A., V.B.-A., S.H., F.P., and V.H. selected patients, characterized allele burdens for MPN driver mutations, and interpreted data on plasma levels of CALR mutants in the context of type of mutation, allele burden, and myeloproliferative neoplasm subtype; A.T., M.E.-K., and C.M. performed megakaryocytic colonies from patients with mutated CALR; I.P. and W.V. supervised and analyzed these experiments; and S.N.C., R.K., W.V., and R.L. planned the research, interpreted data, and wrote the paper.

Conflict-of-interest disclosure: R.K. and S.N.C. and are cofounders of MyeloPro GmbH. The remaining authors declare no competing financial interests.

ORCID profiles: C.P., 0000-0002-8623-3483; N.P., 0000-0001-7869-862X; T.B., 0000-0003-0156-8936; I. Chachoua, 0000-0002-5112-5394; D.V., 0000-0001-7648-8282; A.R., 0000-0002-7297-2920; C.M., 0000-0003-4350-2302; T.E.F., 0000-0003-0251-3865; D.S.M., 0000-0003-1475-6020; I. Casetti, 0000-0001-5232-9543; E.R., 0000-0002-7572-9504; D.P., 0000-0002-6575-8766; M.C., 0000-0001-6984-8817; N.K., 0000-0003-1880-9126; M.A., 0000-0002-3502-5000; R.L., 0000-0002-3322-0080; V.B.-A., 0000-0002-7369-9700; S.H., 0000-0001-8182-990X; I.P., 0000-0002-5915-6910; W.V., 0000-0003-4705-202X; R.K., 0000-0002-6997-8539; S.N.C., 0000-0002-8599-2699.

Correspondence: Stefan N. Constantinescu, Ludwig Institute for Cancer Research Brussels, Ave Hippocrate 74, UCL 75-4, Brussels B-1200, Belgium; email: stefan.constantinescu@bru.licr.org; and Robert Kralovics, Department of Laboratory Medicine, Medical University of Vienna, Anna Spiegel Research Building, Lazarettgasse 14, AKH BT25.2, Level 6, 1090 Vienna, Austria; email: robert.kralovics@meduniwien.ac.at.

Footnotes

Submitted 28 April 2022; accepted 17 October 2022; prepublished online on *Blood* First Edition 10 November 2022. https://doi.org/10.1182/blood.2022016846.

*C.P., N.P., T.B., I. Chachoua, and A.T. are joint first authors.

Data are available on request from the corresponding authors, Stefan N. Constantinescu (stefan.constantinescu@bru.licr.org) and Robert Kralovics (robert.kralovics@meduniwien.ac.at).

The online version of this article contains a data supplement.

There is a *Blood* Commentary on this article in this issue.

The publication costs of this article were defrayed in part by page charge payment. Therefore, and solely to indicate this fact, this article is hereby marked "advertisement" in accordance with 18 USC section 1734.

REFERENCES

1. Nangalia J, Massie CE, Baxter EJ, et al. Somatic CALR mutations in myeloproliferative neoplasms with nonmutated JAK2. *N Engl J Med*. 2013; 369(25):2391-2405.
2. Klampfl T, Gisslinger H, Harutyunyan AS, et al. Somatic mutations of calreticulin in myeloproliferative neoplasms. *N Engl J Med*. 2013;369(25):2379-2390.
3. Michalak M, Groenendyk J, Szabo E, Gold LI, Opas M. Calreticulin, a multi-process calcium-buffering chaperone of the endoplasmic reticulum. *Biochem J*. 2009;417(3):651-666.
4. Chachoua I, Pecquet C, El-Khoury M, et al. Thrombopoietin receptor activation by myeloproliferative neoplasm associated calreticulin mutants. *Blood*. 2016;127(10): 1325-1335.
5. Nivarthi H, Chen D, Cleary C, et al. Thrombopoietin receptor is required for the oncogenic function of CALR mutants. *Leukemia*. 2016;30(8):1759-1763.
6. Elf S, Abdelfattah NS, Baral AJ, et al. Defining the requirements for the pathogenic interaction between mutant calreticulin and MPL in MPN. *Blood*. 2018;131(7):782-786.
7. Elf S, Abdelfattah NS, Chen E, et al. Mutant Calreticulin Requires Both Its Mutant C-terminus and the Thrombopoietin Receptor for Oncogenic Transformation. *Cancer Discov*. 2016;6(4):368-381.
8. Marty C, Pecquet C, Nivarthi H, et al. Calreticulin mutants in mice induce an MPL-dependent thrombocytosis with frequent progression to myelofibrosis. *Blood*. 2016; 127(10):1317-1324.
9. Araki M, Yang Y, Masubuchi N, et al. Activation of the thrombopoietin receptor by mutant calreticulin in CALR-mutant myeloproliferative neoplasms. *Blood*. 2016; 127(10):1307-1316.
10. Balligand T, Achouri Y, Pecquet C, et al. Pathologic activation of thrombopoietin receptor and JAK2-STAT5 pathway by frameshift mutants of mouse calreticulin. *Leukemia*. 2016;30(8):1775-1778.
11. Han L, Schubert C, Kohler J, et al. Calreticulin-mutant proteins induce megakaryocytic signaling to transform hematopoietic cells and undergo accelerated degradation and Golgi-mediated secretion. *J Hematol Oncol*. 2016;9(1):45.
12. Pecquet C, Chachoua I, Roy A, et al. Calreticulin mutants as oncogenic rogue chaperones for TpoR and traffic-defective pathogenic TpoR mutants. *Blood*. 2019; 133(25):2669-2681.
13. Araki M, Yang Y, Imai M, et al. Homomultimerization of mutant calreticulin is a prerequisite for MPL binding and activation. *Leukemia*. 2018;33(1):122-131.
14. Balligand T, Achouri Y, Pecquet C, et al. Knock-in of murine Calr del52 induces essential thrombocythemia with slow-rising dominance in mice and reveals key role of Calr exon 9 in cardiac development. *Leukemia*. 2020;34(2):510-521.
15. Pecquet C, Balligand T, Chachoua I, et al. Secreted mutant calreticulins as rogue cytokines trigger thrombopoietin receptor activation specifically in CALR mutated cells: perspectives for MPN therapy. *Blood*. 2018; 132(suppl 1):4.
16. Liu P, Zhao L, Loos F, et al. Immunosuppression by mutated calreticulin released from malignant cells. *Mol Cell*. 2019; 77(4):748-760.
17. Benlabiod C, Cacemiro MdC, Nédélec A, et al. Calreticulin del52 and ins5 knock-in mice recapitulate different myeloproliferative phenotypes observed in patients with MPN. *Nat Commun*. 2020;11(1):4886.
18. Dupuis M, Schaerer E, Krause KH, Tschopp J. The calcium-binding protein calreticulin is a major constituent of lytic granules in cytolytic T lymphocytes. *J Exp Med*. 1993;177(1):1-7.
19. Eggleton P, Lieu TS, Zappi EG, et al. Calreticulin is released from activated neutrophils and binds to C1q and mannan-binding protein. *Clin Immunol Immunopathol*. 1994;72(3):405-409.
20. Ogden CA, deCathelineau A, Hoffmann PR, et al. C1q and mannose binding lectin engagement of cell surface calreticulin and Cd91 initiates macropinocytosis and uptake of apoptotic cells. *J Exp Med*. 2001;194(6): 781-796.
21. Gardai SJ, McPhillips KA, Frasch SC, et al. Cell-surface calreticulin initiates clearance of viable or apoptotic cells through trans-activation of LRP on the phagocyte. *Cell*. 2005;123(2):321-334.
22. Feng M, Chen JY, Weissman-Tsukamoto R, et al. Macrophages eat cancer cells using their own calreticulin as a guide: roles of TLR and Btk. *Proc Natl Acad Sci U S A*. 2015; 112(7):2145-2150.
23. Beguin Y. Soluble transferrin receptor for the evaluation of erythropoiesis and iron status. *Clin Chim Acta*. 2003;329(1):9-22.
24. Hayes GR, Williams A, Costello CE, Enns CA, Lucas JJ. The critical glycosylation site of human transferrin receptor contains a high-mannose oligosaccharide. *Glycobiology*. 1995;5(2):227-232.
25. Rowland M, Tozer TN. *Exposure and response after a single dose. Clinical Pharmacokinetics/Pharmacodynamics*. Philadelphia: Lippincott Williams and Wilkins; 2005.
26. Thomas GR, Thibodeaux H, Errett CJ, et al. In vivo biological effects of various forms of thrombopoietin in a murine model of transient pancytopenia. *Stem Cells*. 1996; 14(suppl 1):246-255.
27. Zhao X, Feng X, Wu Z, et al. Persistent elevation of plasma thrombopoietin levels after treatment in severe aplastic anemia. *Exp Hematol*. 2018;58:39-43.
28. Wood TJ, Sliva D, Lobie PE, et al. Specificity of transcription enhancement via the STAT responsive element in the serine protease inhibitor 2.1 promoter. *Mol Cell Endocrinol*. 1997;130(1-2):69-81.
29. Wang S, He X, Wu Q, et al. Transferrin receptor 1-mediated iron uptake plays an essential role in hematopoiesis. *Haematologica*. 2020;105(8): 2071-2082.
30. Drachman JG, Millett KM, Kaushansky K. Thrombopoietin signal transduction requires functional JAK2, not TYK2. *J Biol Chem*. 1999;274(19):13480-13484.
31. Michalak M, Corbett EF, Mesaeli N, Nakamura K, Opas M. Calreticulin: one protein, one gene, many functions. *Biochem J*. 1999;344(2):281-292.
32. Kapoor M, Ellgaard L, Gopalakrishnapai J, et al. Mutational analysis provides molecular insight into the carbohydrate-binding region of calreticulin: pivotal roles of tyrosine-109 and aspartate-135 in carbohydrate recognition. *Biochemistry*. 2004;43(1): 97-106.
33. Greenbaum HS, Evers M, Rosencrance A, et al. Type I calreticulin mutations result in hyperactivation of its acetyltransferase function and iron metabolism, inducing a susceptibility to ferroptosis. *Blood*. 2021; 138(suppl 1):3593.
34. Achyutuni S, Nivarthi H, Majoros A, et al. Hematopoietic expression of a chimeric murine-human CALR oncoprotein allows the assessment of anti-CALR antibody immunotherapies in vivo. *Am J Hematol*. 2021;96(6):698-707.